

Original Paper

# Losartan through Hsp70 Avoids Angiotensin II Induced Mesenchymal Epithelial Transition in Proximal Tubule Cells from Spontaneously Hypertensive Rats

Valeria V. Costantino<sup>a,b</sup> Victoria Bocanegra<sup>a,b</sup> Valeria Cacciamani<sup>a</sup>  
Andrea F. Gil Lorenzo<sup>b</sup> María E. Benardon<sup>b</sup> Patricia G. Vallés<sup>a,b</sup>

<sup>a</sup>IMBECU-CONICET (National Council of Scientific and Technical Research of Argentina), Mendoza, Argentina, <sup>b</sup>Área de Fisiopatología, Departamento de Patología, Facultad de Ciencias Médicas, Universidad Nacional de Cuyo, Mendoza, Argentina

## Key Words

Proximal tubule cells • Angiotensin II • Losartan • Hsp70 • Mesenchymal epithelial transition

## Abstract

**Background/Aims:** Renal injury related to hypertension is characterized by glomerular and tubulointerstitial damage. The overactivation of the renin-angiotensin system mainly by angiotensin II (AII) seems to be a main contributor to progressive renal fibrosis. Epithelial to mesenchymal transition (EMT) is a mechanism that promotes renal fibrosis. Owing to heat shock protein 70 (Hsp70) cytoprotective properties, the chaperone exhibits an important potential as a therapeutic target. We investigate the role of Hsp70 on Angiotensin II induced epithelial mesenchymal transition within the Losartan effect in proximal tubule cells (PTCs) from a genetic model of hypertension in rats (SHR). **Methods:** Primary cell culture of PTCs from SHR and Wistar Kyoto (WKY) rats were stimulated with AII, treated with Losartan (L), (L+AII) or untreated (C<sub>0</sub>). The functional Hsp70 role in Losartan effect, after silencing its expression by cell transfection, was determined by Immunofluorescence; Western blotting; Gelatin Zymography assays; Scratch wound assays; flow cytometry; and Live Cell Time-lapse microscopy. **Results:** (L) and (L+AII) treatments induced highly organized actin filaments and increased cortical actin in SHR PTCs. However, SHR PTCs (C<sub>0</sub>) and (AII) treated cells showed disorganized actin. After Hsp72 knockdown in SHR PTCs, (L) was unable to stabilize the actin cytoskeleton. We demonstrated that (L) and (L+AII) increased E-cadherin levels and decreased vinculin,  $\alpha$ -SMA, vimentin, pERK, p38 and Smad2-3 activation compared to (AII) and (C<sub>0</sub>) SHR PTCs. Moreover, (L) inhibited MMP-2 and MMP-9 secretion, reduced migration and cellular

displacement, stabilizing intercellular junctions. Notably, (L) treatment in shHsp72 knockdown SHR PTCs showed results similar to SHR PTCs (C). **Conclusion:** Our results demonstrate that Losartan through Hsp70 inhibits the EMT induced by All in proximal tubule cells derived from SHR.

© 2019 The Author(s). Published by  
Cell Physiol Biochem Press GmbH&Co. KG

## Introduction

Renal injury related to hypertension is characterized by glomerular and tubulointerstitial damage such as tubular atrophy, interstitial fibrosis and periglomerular fibrosis [1]. The damage in renal parenchyma and its vasculature is gradual, evolutive and symptomatically silent. The local overactivation of the renin-angiotensin system mainly by angiotensin II (AII) actions seems to be a main contributor to progressive renal fibrosis through mechanisms participating in the production of profibrotic factors, and extracellular matrix protein production [2]. The physiological and pathological actions of AII are mediated by the AT<sub>1</sub> receptor coupled to the G protein. The molecular mechanisms associated with the receptor activation include the positive regulation of several signaling pathways that involve: reactive oxygen species (ROS) generation, mitogenic kinases (MAP Kinases) activation and small proteins Rho GTPases activation [3, 4]. Oxidative stress plays a critical role in the pathological development of kidney injury related to hypertension [5]. In spontaneously hypertensive rats (SHR), it has been demonstrated gene expression for all main components of phagocyte NADPH oxidase in renal cells, suggesting that the activation of NADPH oxidase within the kidney may precede the development of hypertension [6]. Furthermore, ROS production is the major pathway by which AII induces epithelial mesenchymal transition (EMT) and apoptosis leading to fibrosis [7].

The early signaling events involved in the assembly and structural organization actin cytoskeleton AT<sub>1</sub>R-dependent, include the activation of small Rho GTPase proteins such as RhoA and Rac1. The tubulo-epithelial cells are firmly linked through different adhesion mechanisms. On this way, E-cadherin is a protein present in adherent junctions that binds to intracellular actin filaments and plays a key role preserving the structural integrity of renal epithelia. The initial events in the EMT process include the disruption of epithelial junctional complexes and subsequent loss of cell polarity. Then, a consecutive series of situations lead to cell morphology changes from cuboid to fibroblastic, decreased epithelial proteins expression such as E-cadherin and cytokeratin, cytoskeleton reorganization and increased mesenchymal markers expression, such as vimentin and  $\alpha$ -SMA (smooth muscle actin) [8]. Together, these events define the cell structural change and confers the contractile capacity that allow migration and invasion to other tissue compartments [9, 10]. Another fundamental process involves the disruption of tubular basement membrane by the proteolytic action of metalloproteinases MMP-2 and MMP-9. These metalloproteinases make possible the migration of the transformed cells to the tubular interstitium where their final myofibroblasts morphology is obtained [11]. Several intracellular signaling systems are involved in EMT and renal fibrosis. In the kidney, AII actively participates in renal fibrosis, in part mediated by TGF $\beta$  [12]. Previous studies have demonstrated that the MAPK pathway is required for TGF $\beta$ -mediated EMT and cell migration [13, 14]. In addition, activation of small Rho GTPases is a key step in EMT [15]. Other studies have shown that AII activates the Smad pathway during epithelial mesenchymal transdifferentiation [16-18]. A cell protective mechanism against the ROS effects, include the production of highly conserved proteins called heat shock proteins (Hsp). These molecular chaperones, ubiquitously expressed, help to maintain and restore the normal function of cells against stress, a condition that dramatically increases their expression [19]. Hsp70 regulates a diverse set of signaling pathways through its interaction with proteins [20]. We have focused in the study of the mechanism involved in the antioxidative effect of Losartan, a pharmacological inhibitor of the AT<sub>1</sub> receptor, on the genetic model of hypertension in rats (SHR). Previously, we showed that Losartan induces caveolin-1 and Hsp70 interaction, together with decreased Nox4

protein levels in microdissected proximal tubule membranes [21]. Recently, we determined that Losartan treatment induces increased Hsp70 chaperone expression and decreased oxidative stress through Nox4 protein levels reduction in PTC primary cultures from SHR. The decreased Nox4 was not due to modifications at transcriptional level expression, it was because of the interaction of Hsp70 with its CHIP cochaperone, complex that negatively regulates Nox4 protein levels through proteosomal degradation [22]. These results suggest that Hsp70 plays a key role in the reduction of oxidative stress after the AT1 blockage, being a possible molecular target for therapeutic strategy against hypertensive renal damage.

In regard to this background, here we investigate the Hsp70 role as a modulator of Losartan effect on the cytoskeleton, intercellular junctions stabilization and the epithelial-mesenchymal transition in proximal tubular cells from spontaneously hypertensive rats.

## Materials and Methods

### Reagents

Antibodies against Rac1, RhoA, vinculin, NHE1 and  $\beta$ -actin were purchased from Sigma-Aldrich (St. Louis, MO, USA). Antibodies against E-cadherin, T-FAK, Y397-FAK, phosphor-Smad 2-3 and vimentin were provided by Santa Cruz Biotechnology (Santa Cruz, CA, USA). Secondary antibodies anti-mouse and anti-rabbit were provided by Jackson ImmunoResearch Inc. (West Grove, PA, USA).

### Animals

Spontaneously Hypertensive Rats (SHR) and Wistar-Kyoto (WKY) male rats (8-10 weeks old) were used due to the greater levels of oxidative stress of male SHR compared with female SHR. In this regards, Gillis *et al.* demonstrated that higher oxidative stress in male SHR conduces to a deficiency of Tetrahydrobiopterin ( $BH_4$ ), a critical cofactor required for NO generation, resulting in diminished renal NOS activity [23]. Indirect systolic blood pressure was measured by the tail cuff method prior to perform the experiments, using a pulse sensor photoelectric CCP model in a Grass polygraph model 7 equipped with a 7P8 pre-amplified (Grass Medical Instruments). Tail cuff requires handling, restraint and warming of the animal during measurement, which may cause stress affecting blood pressure and reliability of the results. However, this noninvasive method still provide a useful approach for measurement systolic blood pressure in some experimental circumstances such as detection or screening for frank systolic hypertension or substantial group differences in systolic blood pressure [24-26]. The average of 3 blood pressure readings and body weight were recorded in twelve animals of each group. Three independent experiments were performed. Body weight and systolic blood pressure are included in Table 1. All animals were cared in accordance with the Guiding Principles in the Care and Use of Animals of the US National Institute Health. All procedures were approved by the Institutional Committee of Animal Care and Use from the School of Medicine, Universidad Nacional de Cuyo, Argentina. (Protocol approval N° 75/2016). All surgery proceeding were performed under ketamine/xylazine (50 mg/kg and 2 mg/kg respectively) anesthesia, and all efforts were made to minimize animal suffering.

### Cell Culture

The isolation of proximal tubule cells (PTCs) from SHR and WKY rats was performed as previously described [27, 28] with some modifications. Briefly, kidneys were excised and the cortex was separated. Fragments of renal cortex were desegregated and placed in ice cold Krebs-Henseleit solution (KHS) pH 7.4 and incubated with 95% O<sub>2</sub>/5% CO<sub>2</sub> at 37 °C for 60 min. This suspension was centrifuged (60 g), the supernatant was discarded and the pellet re-suspended in ice cold KHS for thrice. Then, the pellet was re-suspended in 30 ml of ice cold Percoll 50% solution in KHS and centrifuged for 30 min at 4 °C at 15.000 rpm on a Beckman Coulter centrifuge (Beckman Coulter, Inc, CA, USA). The fourth fraction was re-suspended in

**Table 1.** Body weight and blood pressure in WKY and SHR rats. The average of 3 blood pressure readings and body weight were recorded in 12 animals of each group. Three independent experiments were performed

Parameter	WKY	SHR	p
Body Weight (g $\pm$ SEM)	158.54 $\pm$ 8.02	102.89 $\pm$ 7.45	<0.001
Blood Pressure (mmHg $\pm$ SEM)	112.25 $\pm$ 2.35	165.85 $\pm$ 3.33	<0.001

ice-cold KHS, washed 3 times as previously described and then re-suspended in DMEM F12 supplemented with 20% SFB. Cells were cultured with culture medium (DMEM F12 containing 1% penicillin/ streptomycin and 10% SFB), at 37 °C under 5% CO<sub>2</sub> in a humidified atmosphere. Cells were identified as PTCs by positive staining antibody against Megalin (Supplementary Fig. S1A – for all supplemental material see [www.cellphysiolbiochem.com](http://www.cellphysiolbiochem.com)).

PTCs from SHR and WKY rats were stimulated with Angiotensin II (100 nM) (AII), treated with Losartan (10 µM) (L) or with Losartan plus Angiotensin II in the same concentrations (L+AII) for 24 h. Non-treated cells were used as control (C<sub>0</sub>).

### *Flow Cytometry*

Flow cytometry analysis was performed to determine PTCs primary cell culture purity. PTCs were resuspended in fixation/permeabilization solution (BD Cytofix/Cytoperm, Bioscience), incubated with Aqp-2 and Megalin antibodies. Then, PTCs were incubated with the secondary antibody conjugated with APC and FITC respectively and analyzed by flow cytometry. For each assay, at least 20000 cells were analyzed. FC analysis was performed with a FACS Aria III cytometer (BD Bioscience). Data were analyzed with the FACSDIVA software (BD Bioscience). Controls included isotype-matched unspecific MoAbs used as negative controls. Flow cytometry analysis showed a 71.3% of PTCs expressing Megalin and 0.23% of Aqp-2 positive cells. The purity of the kidney PTCs primary cell culture is reflected from the percentage of the cell population Megalin positive (Supplementary Fig. S1B).

### *Cell Transfection*

Cell transfection assays were performed as described [22]. Briefly, for knockdown of Hsp72 expression, transient transfections were done with 2 µg/ml shHsp72-pSIREN-RetroQ vector and/or pSIREN-RetroQ empty vector (ev) (Mock-transfection control) for 48 h using Lipofectamine™2000 (Invitrogen, Carlsbad, CA) according to manufacturer's recommendations. The shHsp72-pSIREN-RetroQ vector was generously provided by Dr. MY Sherman (Boston University Medical School, Boston, MA, USA). The vector contained the sequence of human Hsp72 as target for RNA interference: shHsp72 GAAGGACGAGTTTGAGCACAA (start 1961). No differences were shown between transfected empty vector cells and non-transfected cells. The transfection efficiency was evaluated in each experiment using pSIREN-DsRed-Express. After 48 h of transfection, cells were treated with AII or Losartan as previously described. The efficiency of Hsp72 silencing was analyzed by western blot (Supplementary Fig. S1C).

### *Immunostaining and Confocal Immunofluorescence Microscopy*

The PTCs were plated on coverslips and treated as described previously. The cells were fixed in 4% paraformaldehyde, washed with PBS and blocked with 50 mM NH<sub>4</sub>Cl, permeabilized with 0.05% saponin/0.5% BSA in PBS and incubated over night with primary antibodies as mentioned below. After, the cells were washed and incubated for 1 h with secondary antibodies fluorophores conjugated. Whole nuclei were visualized using Hoechst. The primary antibodies against β-actin, vinculin, e-cadherin were used in a 1:100 dilution. The secondary antibodies used were Cy3-conjugated anti-mouse or Alexa 488-conjugated anti-rabbit in a 1:3000 dilution. Images were obtained with an Olympus FV1000, (Olympus, Tokyo, Japan). The specificity of the immunostaining was evaluated by omission of the primary antibody. At least 50 cells were examined using Mac Biophotonics Image J software in each group in three independent experiments.

### *Protein Purification and Immunoblot Analysis*

Western blot analysis was performed in the plasma membrane and cytosolic fractions. Fractions were obtained as described [29]. Equal amounts of proteins were separated by SDS-PAGE and transferred into nitrocellulose membranes (BioRad Laboratories, Hercules, CA, USA). The membranes were blocked and blotted with primary antibodies overnight at 4°C. Subsequently, membranes were incubated with the appropriate horseradish peroxidase-conjugated secondary antibodies for 2 h, at room temperature. A SuperSignal West Pico chemiluminescent substrate kit (Pierce/ThermoFisher Scientific Inc., Rockford, IL, USA) was used to visualize protein bands. Band densities were determined using the Image J program.

### *Gelatin Zymography assays*

Zymographic analysis of the MMP proteolytic activity in cultured cell supernatants was performed according to the method previously described [30, 31]. Briefly, an equal volume of PTCs extract was grown on 60 mm plates to 80% confluence. Subsequently, culture medium was changed to 1.5 ml and the different treatments were added to the cultures for 24 h. Later, the conditioned media was collected and centrifuged at 13,000 for 5 min to remove any cell debris. The protein concentration was determined using Bradford method. Constant amount of protein from the conditioned media was loaded into 10% SDS-polyacrylamide gel containing 1 mg/ml gelatin (Bio-Rad). After electrophoresis, SDS was removed from the gel by incubation in 2.5% Triton X-100 at room temperature for 30 minutes with gentle shaking. The gel was well washed with distilled water to remove detergent and incubated at 37°C for 16 to 36 hours in a developing buffer containing 50 mmol/L Tris-HCl, pH 7.6, 0.2 mol/L NaCl, 5 mmol/L CaCl<sub>2</sub> and 0.02% Brij 35. Then, the gel was stained with a solution of 30% methanol, 10% glacial acetic acid, and 0.5% Coomassie Blue G250, followed by de-staining in the same solution without dye. Proteinase activity was detected as unstained bands on a blue background representing areas of gelatin digestion.

### *Scratch wound assays*

The cell migration was assessed in scratch wound assays. Confluent monolayers of PTCs serum starved for 24 h were wounded using a micropipette tip (200 µl yellow tip), rinsed twice to remove nonadherent cells with growth medium and treated as mentioned above. The wound closure was monitored for 24 h and photographed using a Nikon Eclipse 80i microscopy (Nikon Corp., Tokyo, Japan). The wound healing area was analyzed using Image J software (Rasband WS, Image J. Bethesda, MD: National Institutes of Health: 28 October 2003. <http://rsbweb.nih.gov/ij/>) and % of area reduction at 24h was quantified. These experiments were repeated thrice with similar results using different cell isolations.

### *Live Cell Time-lapse Microscopy and Analysis*

Phase-contrast time-lapse microscopy was performed as described [32]. Briefly, PTCs were grown on 60 mm plates to 60% confluence and treated as mentioned above. Following, the cells for each condition were recorded using a Nikon Eclipse TE 2000 U motorized inverted microscope (Nikon Corp., Tokyo, Japan) with an incubation chamber (37°C, 5% CO<sub>2</sub>) and a Hamamatsu ORCA-ER cooled CCD camera (Hamamatsu Photonics, Tokyo, Japan). Images were acquired every 15 min for 16 h. Time-lapse videos were reviewed, and the cell displacement and movement rate were determined using the Image J software program. The photographic sequence was made in 50 different cells for each condition in three independent experiments.

### *Statistical Analysis*

Data are presented as means ± SEM from at least 3 independent experiments. Groups were compared using one-way analysis of variance (ANOVA). Bonferroni post hoc test was used to compensate for multiple testing procedures at as  $p < 0.05$  significant level, using Prism 5 program (GraphPad Software Inc., La Jolla, CA, USA).

## Results

### *Losartan stabilizes the actin cytoskeleton through Hsp70*

The actin cytoskeleton plays a crucial role in PTCs since it is involved in polarity maintenance, barrier function, microvilli structure and extracellular matrix adhesion. In order to analyze Hsp70 participation in the Losartan effect on cytoskeleton integrity from SHR PTCs, we evaluated the distribution of F-actin by immunofluorescence. Rac1 and RhoA activation was evaluated by western blot in membrane fractions. Therefore, SHR PTCs or shHsp72 knockdown SHR PTCs were examined in the presence of serum (C<sub>c</sub> or C<sub>sh</sub>), Angiotensin II (AII), Losartan (L) and Losartan plus Angiotensin II (L+AII). PTCs from WKY rats (WKY PTCs C) were used as normotensive controls. As shown in the upper panel of Fig. 1A, in SHR PTCs (C<sub>c</sub>) and (AII) treated SHR PTCs actin was found forming numerous long and thick cytosolic stress fibers spanning the entire cross-sectional area from the cells and showing protrusions (lamella) on the leading edge in most of the cells (inset). However, in

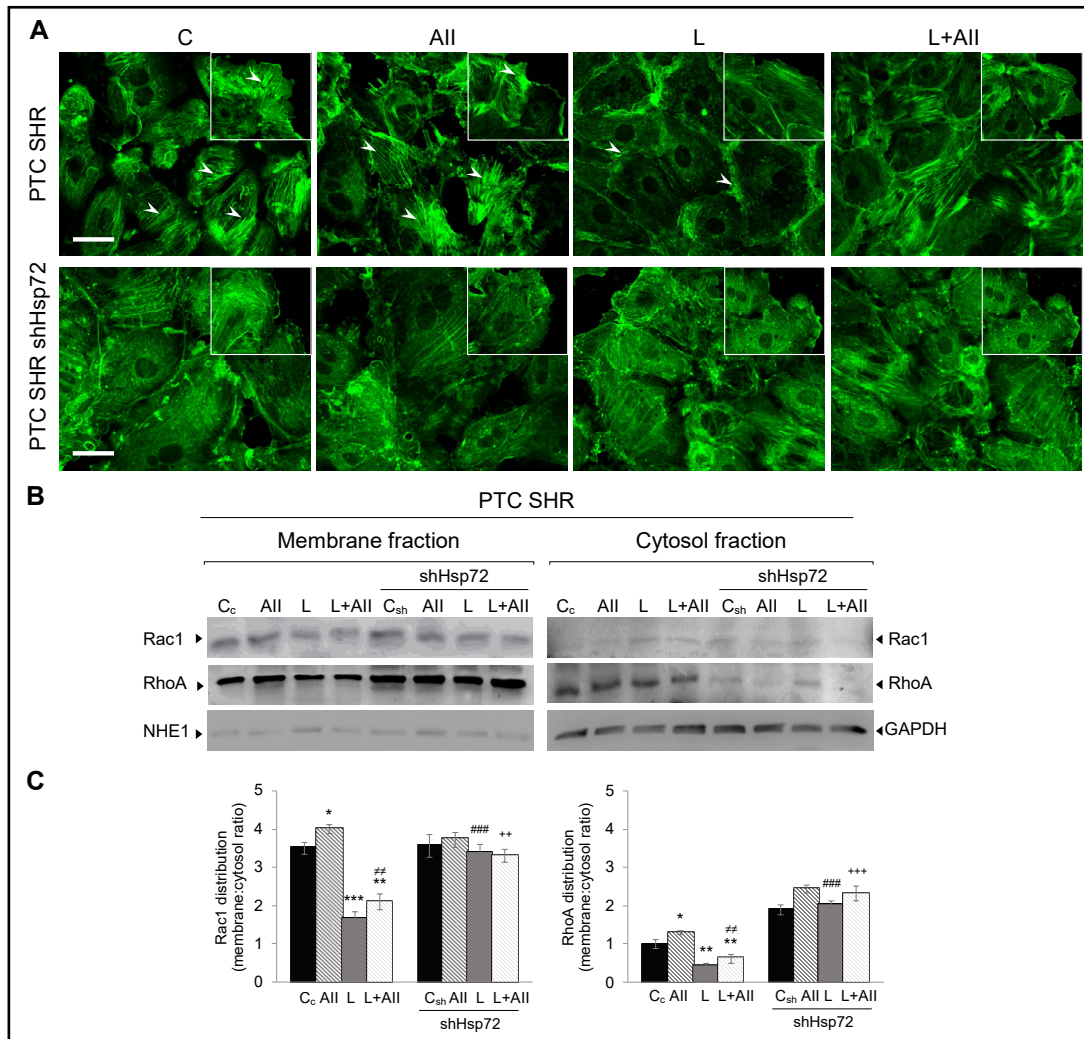


**Fig. 1.** Analysis of Hsp70 within the Losartan effect on PTCs cytoskeleton stabilization. A) SHR PTCs (upper panel) or shHsp72 Knockdown SHR PTCs (lower panel) cells were subjected to different treatments: Control (C<sub>c</sub> or C<sub>sh</sub>), Angiotensin II (AII), Losartan (L) or Losartan plus Angiotensin II (L+AII). To visualize actin cytoskeleton, the cells were stained with anti-β actin and analyzed by immunofluorescence. Fluorescence micrographs show actin cytoskeleton (white arrowheads). Inset: cells stained show protrusions at the leading edge (top right). Pictures display representative areas of staining from 3 independent experiments. Bar: 50 μm. B) Relative abundance of Rac1 and RhoA on SHR PTCs and shHsp72 knockdown SHR PTCs in membrane and cytosol fractions was determined by Western blotting. Cells were subjected to different treatments. NHE1 and GAPDH were used as membrane and cytosol loading control respectively. C) Band intensities were quantified by densitometric analysis and data are expressed as membrane-to-cytosolic ratios. Bars means ± SEM, n=3. \*p<0.05; \*\*p<0.01; \*\*\*p<0.001 vs SHR PTCs control group (C<sub>c</sub>). ### p<0.01; ### p<0.001 vs SHR PTCs (L). \*\* p<0.01 vs SHR PTCs (AII). \*\* p<0.01; \*\*\* p<0.001 vs SHR PTCs (L+AII).

(L) treated SHR PTCs, actin microfilaments were organized as a circumferential network around the periphery of the cell, at cell-cell contact, with decreased lamella formation. We also observed that Losartan decreases stress fiber in cells treated with (AII). To determine the Hsp70 involvement in Losartan effect, SHR PTCs were transfected to transiently silence Hsp72 expression (inducible fraction of Hsp70) and then, exposed to the different treatment. When Hsp72 expression was silenced (Fig. 1A lower panel), Losartan was not able to stabilize the cytoskeleton, showing an increase in misaligned actin filaments and lamella formation. Western blot assay showed that (AII) treatment increased Rac1 and RhoA

protein levels by 14.8% and 31.4% at membrane fractions respectively, while (L) treatment decreased these protein levels by 47.6% and 58.3% respectively, both groups compared to SHR control cells (C<sub>0</sub>) (defined as 100%). When the cells were treated with (L+AII), Rac1 and RhoA, protein levels decreased by 60.1% and 38.2% related to SHR control, respectively (Fig. 1B, C). Thus, Losartan abolished the AII effect on Rac1 and RhoA activation. However, in SHR PTCs shHsp72 knockdown, treatment with (L) and (L+AII) did not reduce both GTPases activation compared to non-transfected SHR PTCs treated with (L) and (L+AII), these results are consistent with the one obtained by immunofluorescence.

*Losartan inhibits the focal adhesions formation and stabilizes the intercellular junctions through Hsp70*

To assess whether these changes on cytoskeletal organization also correlated with the one in focal adhesion, we next examined focal adhesions with vinculin staining in proximal tubule cells. (AII) treated SHR PTCs displayed an increased vinculin staining in central and peripheral focal adhesions whereas (L) and (L+AII) treated SHR PTCs showed a marked reduction on vinculin staining when compared to SHR PTCs (C<sub>0</sub>) (Fig. 2A upper panel and B). In contrast, in (L) and (L+AII) treated shHsp72 knockdown SHR PTCs, after vinculin staining, we demonstrated a significant increase of central and peripheral focal adhesions compared to non-transfected (L) and (L+AII) treated SHR PTCs (Fig. 2A lower panel and B). Next, we stained these cells with anti-E cadherin to visualize cell-cell contact. Staining of (L) and (L+AII) treated SHR PTCs demonstrated higher E-cadherin expression in both cytosol and cell periphery at sites of cell-cell contact, whereas (AII) treated SHR PTCs showed decreased E-cadherin staining compared to SHR PTCs (C<sub>0</sub>) (Fig. 2C upper panel and D). The E-cadherin staining on (L) and (L+AII) treated shHsp72 knockdown SHR PTCs demonstrated a discontinuous pattern without increase on cortical E-cadherin expression (Fig. 2C lower panel and D). Western Blot analysis showed increased vinculin protein levels by 27.33% in (AII) treated SHR PTCs without significant differences in E-cadherin protein levels compared to SHR PTCs (C<sub>0</sub>). However, the (L) and (L+AII) treatment decreased vinculin levels by 36.56% and 19.43% respectively; and increased E-cadherin protein levels by 104.15% and 77.01% respectively, compared with SHR PTCs (C<sub>0</sub>). Nevertheless, in shHsp72 knockdown SHR PTCs we observed increased vinculin levels and decreased E-cadherin levels in all treatment, which is consistent with our results from the immunofluorescence study, (Fig. 2E).

Further, we analyzed the levels of focal adhesion kinase (FAK) phosphorylation/activation involved in the signal transduction pathways that promote migration. We observed that (AII) treated SHR PTCs induced a 23.53% increase on phosphorylated FAK levels, while, the (L) and (L+AII) treated SHR PTCs led to a reduction on phosphorylated FAK levels by 33.08% and 10.58%, when compared to SHR PTCs and (C<sub>0</sub>) respectively. Furthermore, (L) and (L+AII) shHsp72 knockdown SHR PTCs showed higher phosphorylated FAK levels similar to SHR PTCs control (Fig. 2E). These results allow us to suggest that Hsp70 chaperone is involved in the Losartan effect on cytoskeleton stabilization, focal adhesion complexes decrease and maintenance of intracellular junction in PTCs from SHR.

*Hsp70 involvement in the inhibition of the mesenchymal markers induced by Losartan*

To evaluate if Hsp70 is included within the Losartan effect on EMT, we examined the de novo expression of  $\alpha$ -SMA and vimentin, phenotypic markers for myofibroblast cells, in SHR PTCs by western blot. The (AII) treated SHR PTCs showed no significant differences in these phenotypic markers levels, while, (L) treatment induced a 51.21% and 47.77% decrease in  $\alpha$ -SMA and vimentin protein levels compared to SHR PTCs (C<sub>0</sub>), respectively. The (L+AII) treatment showed a slight decrease in  $\alpha$ -SMA and vimentin protein levels by 17.95% and 20.54% related to SHR PTCs (C<sub>0</sub>), respectively (Fig. 3A, B). Although the (L+AII) treatment, was not robust as (L) treatment, significant differences were observed related to SHR PTCs (C<sub>0</sub>) and (AII) treated SHR PTCs. In contrast, in shHsp72 knockdown SHR PTCs, Losartan treatment could not decrease the level of these proteins (Fig. 3A, B). Considering that the EMT induction is accompanied by an

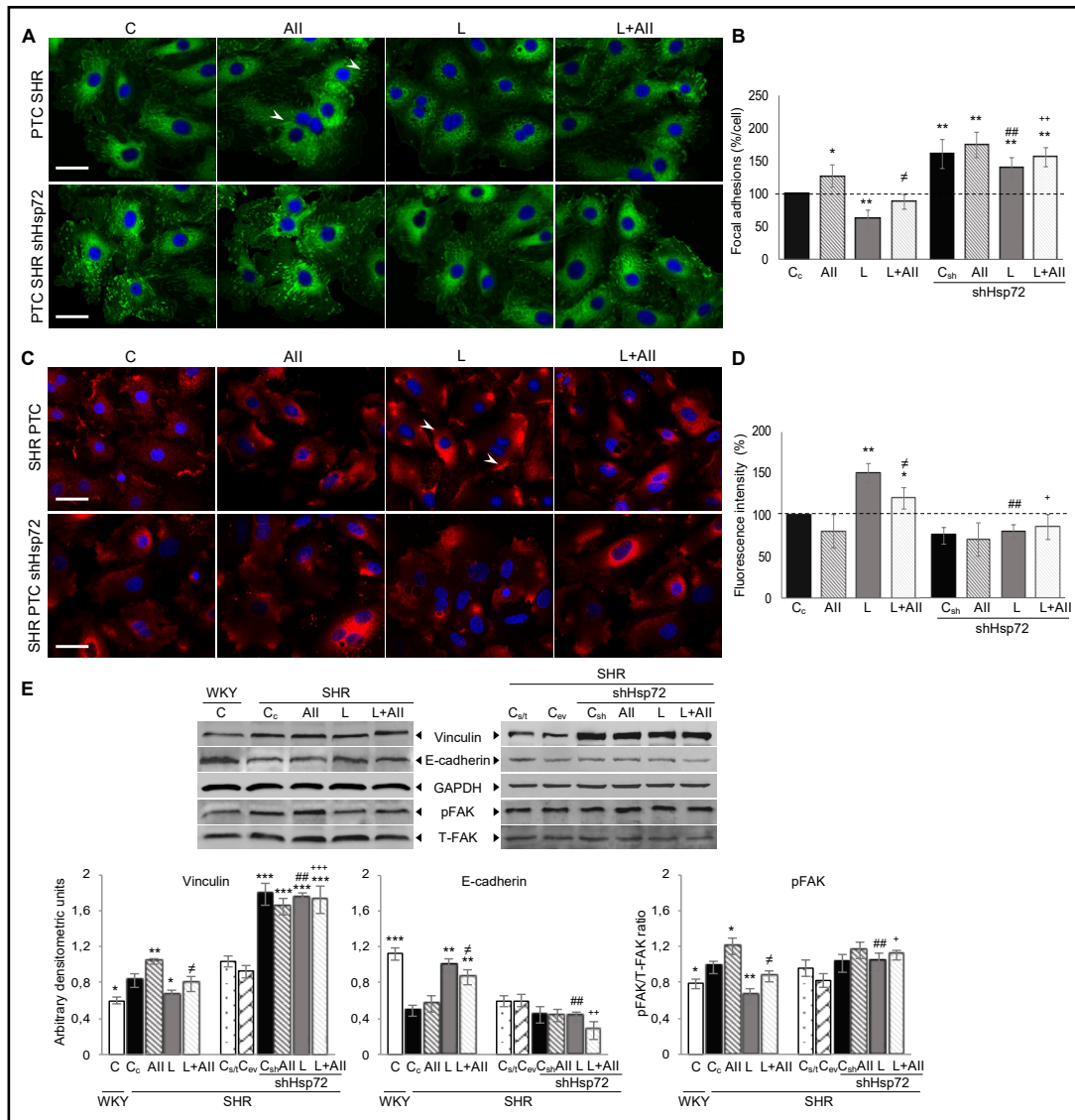


**Fig. 2.** Hsp70 involvement in the Losartan effect on focal adhesions and junction cell stabilization. SHR PTCs or shHsp72 Knockdown SHR PTCs were subjected to different treatments: Control (C<sub>c</sub> or C<sub>sh</sub>), Angiotensin II (AII), Losartan (L) or Losartan plus Angiotensin II (L+AII). To visualize focal adhesions and analyze the distribution of intercellular adhesion molecule E-cadherin, the cells were stained with anti-vinculin and with anti-E-cadherin respectively and analyzed by immunofluorescence. A) Fluorescence micrographs show focal adhesions (white arrowheads) of SHR PTCs (upper panel) or shHsp72 knockdown SHR PTCs (lower panel). B) Quantification percentage of focal adhesions per cell. C) Fluorescence micrographs show the distribution of E-cadherin (white arrowheads) in SHR PTCs (upper panel) or shHsp72 knockdown SHR PTCs (lower panel). D) Quantification of the fluorescence intensity on the cell periphery. Pictures display representative areas of staining from 3 independent experiments. Bar: 50 μm. The data are expressed as a percentage relative to the SHR PTCs control (defined as 100%). At least 70 cells were analyzed for each treatment in three independent experiments. E) Immunoblot analysis of Vinculin, E-cadherin, pFAK and T-FAK in total fractions from SHR PTCs, shHsp72 Knockdown SHR PTCs subjected to different treatments and SHR PTCs empty vector transfected (C<sub>ev</sub>) or non-transfected (C<sub>s/t</sub>). GAPDH was used as loading control. Band intensities were quantified by densitometric analysis. The phosphorylation of FAK was normalized to total protein expression. Bars means ± SEM, n=3. \*p<0.05; \*\*p<0.01; \*\*\*p<0.001 vs SHR PTCs control group (C<sub>c</sub>). ##p<0.01 vs SHR PTCs (L). #p<0.05 vs SHR PTCs (AII). + p<0.05; \*\* p<0.01; \*\*\* p<0.001 vs SHR PTCs (L+AII).

increased expression of MMP-2 and MMP-9 then, we evaluate the proteolytic activity of these enzymes. The zymographic analysis of conditioned media exhibited that (L) treatment induced a marked decrease on MMP-9 and MMP-2 secretion by 51.80% and 40% compared to SHR PTCs (C<sub>0</sub>), respectively. PTCs from SHR group treated with (L+AII) exhibited reduced MMP-9 and MMP-2 secretion by 10.56% and 20%, showing significant differences related to (AII) treated SHR PTCs. In shHsp72 knockdown SHR PTCs Losartan was not able to inhibit the secretion of these metalloproteinases (Fig. 3C, D). Western blot analyses confirm the MMP-9 decrease in (L) and (L+AII) treated SHR PTCs and the increase in MMP-9 expression in all treatment after silencing Hsp72 (Fig. 3A).

Next, by western blot we analyze activation of intracellular signaling systems involved in the ETM regulation. The (AII) treatment of SHR PTCs showed increased phosphorylated MAPK pp38 by 24.93% and pERK1/2 by 23.82% protein levels however, the (L) treatment significantly decreased both phosphorylated kinases protein levels by 43.98% and 27.55% compared to SHR PTCs (C<sub>0</sub>) respectively. The (L+AII) treatment showed a reduction of 21.33% in pp38 protein levels, but no significant differences were found in pERK protein levels related to SHR PTCs (C<sub>0</sub>). Nevertheless, this treatment showed a significant decrease on pp38 and pERK compared to (AII) treated SHR PTCs. In addition, the (L) and (L+AII) treatments showed a significant decrease on phosphorylated Smad 2/3 by 37% and 16.40%, respectively and in the transcription factor Snail1 expression by 47.33 % and 28.34%, respectively compared to SHR PTCs (C<sub>0</sub>). Snail is a target gene of Smad 2/3 activated that promote the repression of E-cadherin. When the Hsp72 expression was silenced, an increased level of these proteins was observed in all treatment, (Fig. 3E, F). These results allow us to suggest that Hsp70 could be involved in the Losartan effect on EMT.

#### *Hsp70 is involved in the inhibitory effect of Losartan on EMT-induced cell migration*

Morphological cytoskeletal cell changes involved in cell migration are pivotal to the EMT process. In this context, we examined proximal tubule cells migration using a scratch wound assay. The wound closure percent was 20.18% in SHR PTCs (C<sub>0</sub>) compared to 10.48% of the WKY PTCs (C), indicating that migration capacity in SHR PTCs was higher than in WKY. (AII) stimulated migration of SHR PTCs showed a wound closure percent of 29.02% while (L) and (L+AII) treated SHR PTCs showed wound closure percent of 12.76% and 17.78 % respectively (Fig. 4A, C). These results reveal that (L) treatment inhibits the SHR PTCs migration. Nevertheless, as shown in Fig. 4B, C (L) and (L+AII) treated shHsp72 knockdown SHR PTCs were not able to decrease the wound closure. This indicates that Losartan, through Hsp70, inhibits the AII effect on cell migration induced by EMT.

#### *Hsp70 mediates the Losartan effect on cell morphology and displacement*

Further, we examined cell displacement and movement velocity through live cell time-lapse microscopy. As observed in Fig. 5A, D, WKY PTCs (C) showed lower movement rate by 41.78% and cell displacement by 42.13% related to SHR PTCs (C<sub>0</sub>) (Fig. 5B, D). AII stimulated SHR PTCs induced an increase of 11.88% and 17.73% in both parameters vs SHR PTCs (C<sub>0</sub>), respectively. The (L) and (L+AII) treated SHR PTCs showed a significant decrease on displacement by 53.36% and 36.09% respectively; and movement rate by 44.69 and 30.18% respectively, compared to SHR PTCs (C<sub>0</sub>) (Fig. 5B, D), showing values similar to the one of the WKY PTCs (C). However, (L) treated shHsp72 knockdown SHR PTCs showed velocity and displacement values that resemble those of the SHR PTCs (C<sub>0</sub>) (Fig. 5C, D) indicating that after the Hsp72 silencing, Losartan treatment did not inhibit cell displacement. No differences were shown between WKY PTCs with and without Losartan treatment, data not shown. This assay also showed that in the SHR PTCs (C<sub>0</sub>) the intercellular junctions were affected, evidenced by changes in cell morphology and loss of cell-cell contact. However, in (L) and (L+AII) treated SHR PTCs the intercellular junctions showed a behavior similar to the one of WKY PTCs (C). In (L) treated shHsp72 knockdown SHR PTCs, morphological

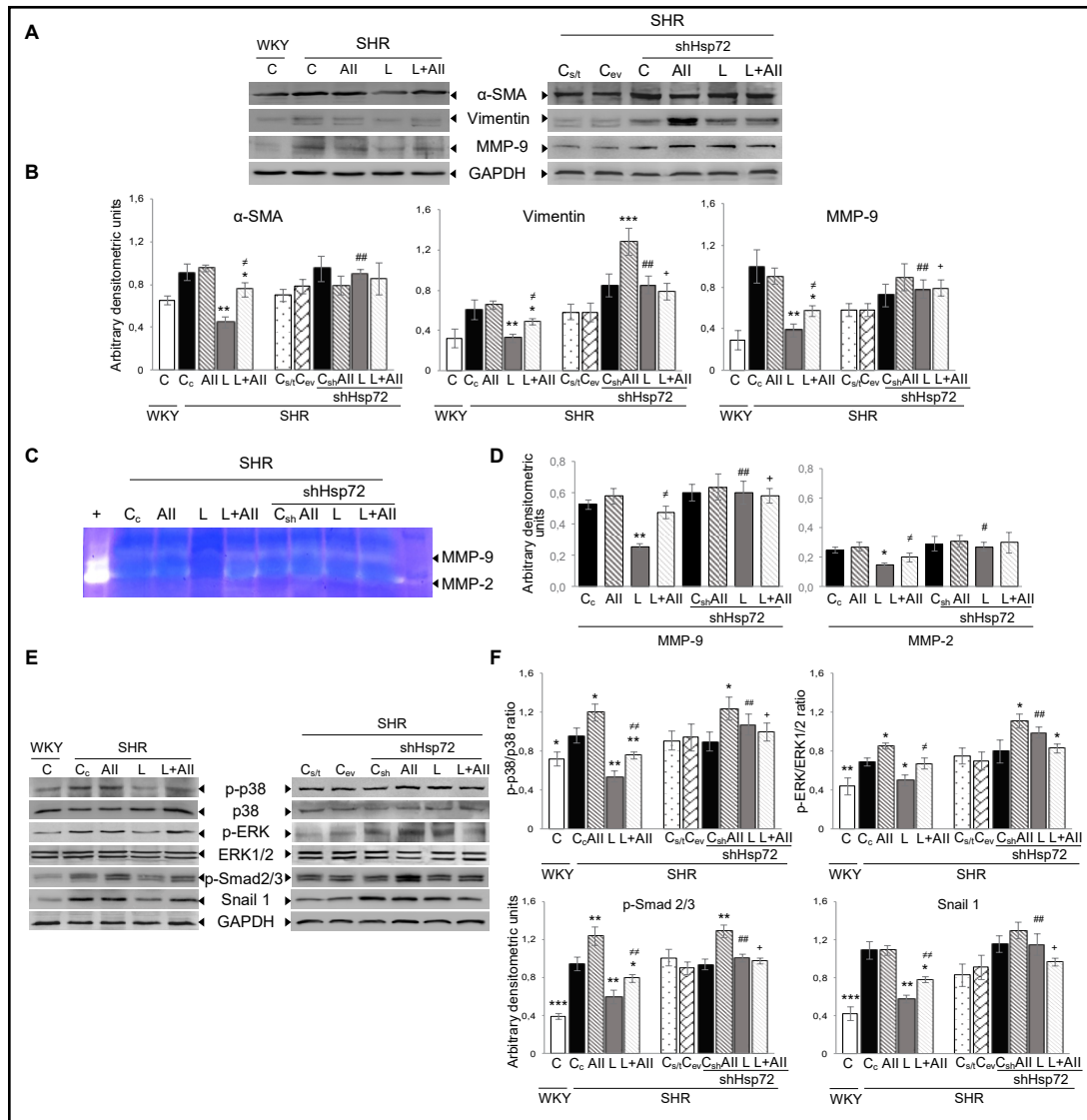


**Fig. 3.** Hsp70 under the Losartan effect in the expression of mesenchymal markers. Immunoblot analysis of A)  $\alpha$ -SMA, vimentin and MMP-9 in total fractions from SHR PTCs and shHsp72 Knockdown SHR PTCs. Cells were subjected to different treatments: Control (C<sub>c</sub> or C<sub>sh</sub>), Angiotensin II (AII), Losartan (L) or Losartan plus Angiotensin II (L+AII) and SHR PTCs empty vector transfected (C<sub>ev</sub>) or non-transfected (C<sub>s/l</sub>). GAPDH was used as loading control. Representative images of 3 independent experiments are shown. B) Band intensities were quantified by densitometric analysis. C) Zymographic analysis of the conditioned media derived from SHR PTCs and shHsp72 Knockdown SHR PTCs subjected to different treatments is shown. Samples equalized for protein content were separated on a 10% SDS-polyacrylamide gel containing 0.1% gelatin. Proteolytic activity was demonstrated by digestion of gelatin, resulting in the bands of clearing. The locations of bands corresponding to MMP-2 and MMP-9 are indicated. D) Band intensities were quantified by densitometric analysis. Immunoblot analysis of E) p-p38, p38, p-ERK, ERK 1/2 p-Smad 2/3 from SHR PTCs and shHsp72 Knockdown SHR PTCs total fractions. Cells were subjected to different treatments. GAPDH was employed as loading control. Representative images of 3 independent experiments are shown. B) Band intensities were quantified by densitometric analysis. Bars means  $\pm$  SEM, n=3. \*p $\leq$ 0.05; \*\*p $\leq$ 0.01; \*\*\*p $\leq$ 0.001 vs SHR PTCs control group (C<sub>c</sub>). #p $\leq$ 0.05, ##p $\leq$ 0.01 vs SHR PTCs (L). \* p $\leq$ 0.05, \*\* p $\leq$ 0.01 vs SHR PTCs (AII). + p $\leq$ 0.05; \*\*p $\leq$ 0.01 vs SHR PTCs (L+AII).

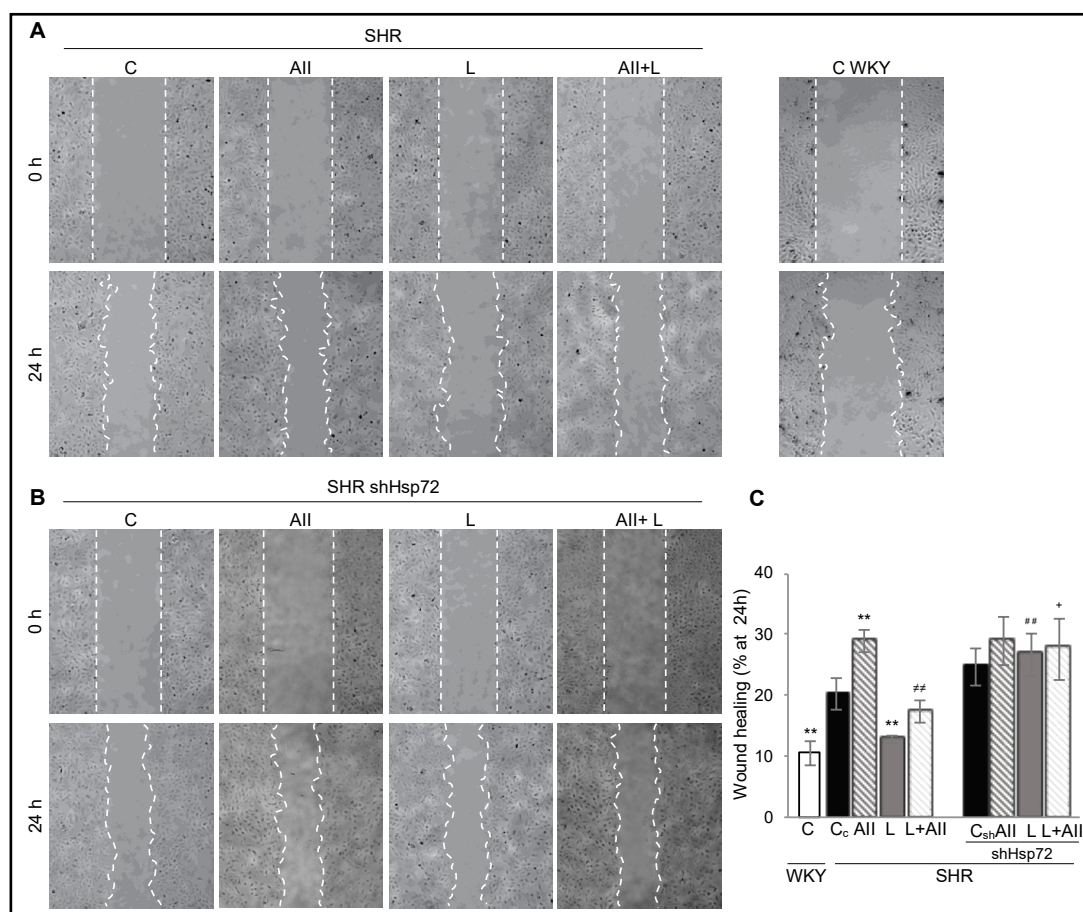


**Fig. 4.** The Losartan effect on PTCs migration. Hsp70 participation. Scratch wound assay. A) WKY or SHR PTCs and B) SHR PTCs shHsp72 Knockdown were grown to confluence, wounded with a P100 pipette tip and subjected to different treatments. Photomicrographs were taken after 0 and 24 h of incubation. WKY PTCs were used as normotensive controls. C) Wound closure quantification. Bars means  $\pm$  SEM, n=3. \*\*  $p \leq 0.01$  vs SHR PTCs (C<sub>c</sub>); ##  $p \leq 0.01$  vs SHR PTCs (L). \*\*  $p \leq 0.01$  vs SHR PTCs (AII). +  $p \leq 0.05$  vs SHR PTCs (L+AII).

changes and intercellular junction's loss were observed after 4 h and continued to be accentuated as time goes by. These results show that Losartan effect on cell adhesion and migratory properties may be mediated by the Hsp70 chaperone. Taken together, these data suggest that in hypertensive rats, Losartan inhibits the tubular epithelial cells conversion into myofibroblasts induced by AII, and Hsp70 is involved in this process.

## Discussion

In this study, we demonstrated that Losartan avoids the epithelial mesenchymal transition induced by AII and we characterize the Hsp70 chaperone as an important mediator of the Losartan effect which entail migration reduction and cytoskeletal stabilization in proximal tubule cells. We focus on this chaperone as a potential target that ameliorates renal damage produced by hypertension. Our results indicate that Hsp70 under the AT<sub>1</sub> receptor blockage, is involved in the cellular response by inducing decreased pre-fibrotic factors that intervene in the mesenchymal epithelium transition. Although most of the antioxidative effects of Losartan have been reported, a direct link between the Hsp70 chaperone and the epithelial-mesenchymal transition (EMT) has not been widely studied in proximal tubule cells.

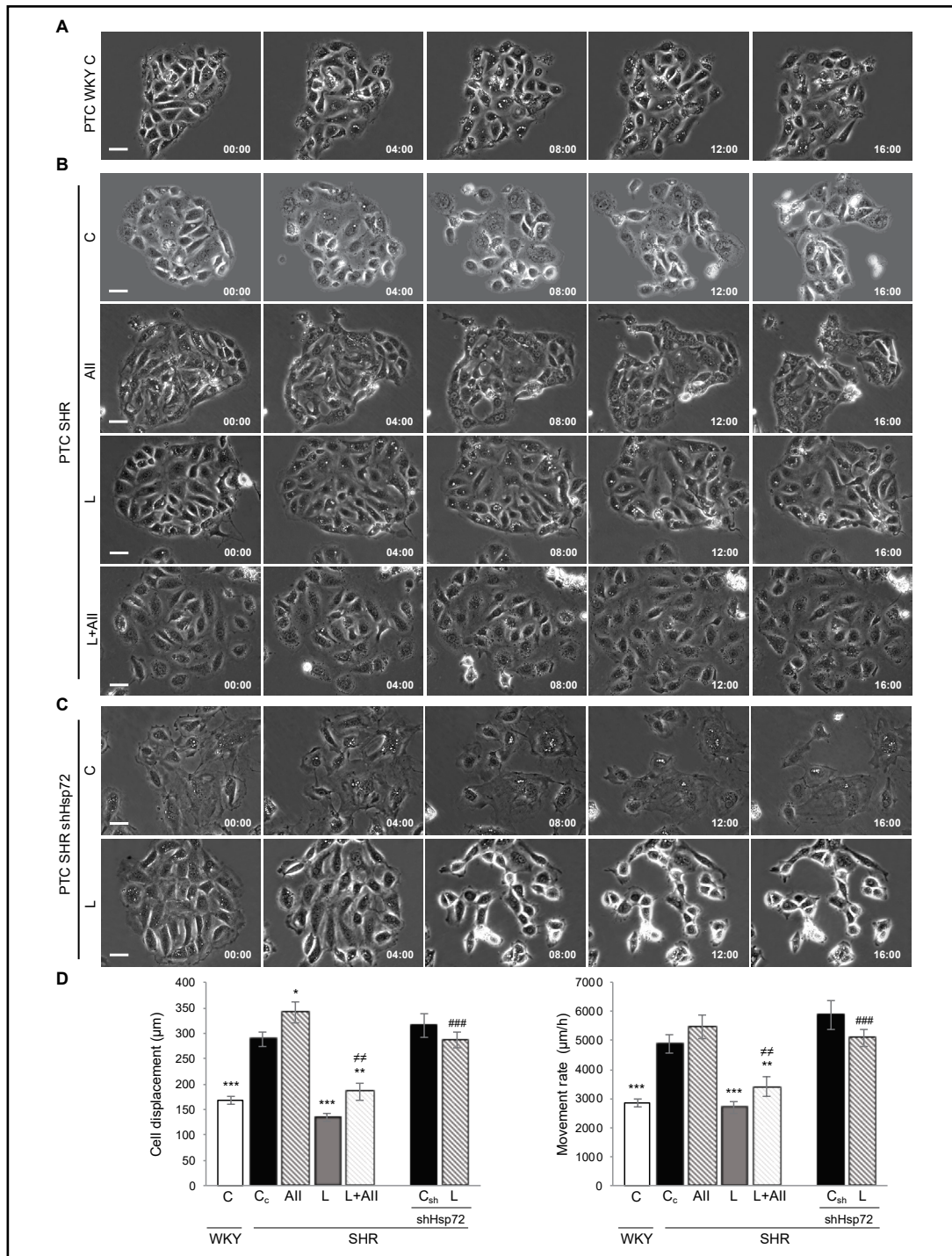


**Fig. 5.** Hsp70 within the Losartan effect on PTCs displacement and movement rate. Live cell time-lapse microscopy assay. PTCs were subjected to different treatments and analyzed by phase contrast in live time-lapse microscopy from 0 to 16 h treatment; images were acquired every 15 min using a Nikon Eclipse TE 2000-U inverted microscope. Representative images of A) WKY PTCs (C), B) SHR PTCs (C<sub>c</sub>), (AII), (L) and (L+AII) treated cells or C) shHsp72 knockdown SHR PTCs (C<sub>sh</sub>) and (L) treated at the beginning of treatment (00:00) to 16 h. Lower right of each panel: average time (h:min). Bar: 50 µm. The average of cell displacement and movement rate (D) were calculated by analyzing 3 movies, by following 60 cells in each treatment condition. Bars means ± SEM, n=3. \*p<0.05; \*\* p<0.01, \*\*\* p<0.001 vs SHR PTCs control group (C<sub>c</sub>). ### p<0.001 vs SHR PTCs (L). \*\* p<0.01 vs SHR PTCs (AII).

Previous work supports that EMT is involved in renal pathogenesis, particularly in renal fibrosis [33, 34]. EMT also plays an imperative role in renal interstitial fibrosis in diabetic nephropathy [35]. The RAS overactivation is an important contributor to the pathogenesis of hypertension and profibrotic events that leads to EMT and the progression of chronic kidney disease [36]. AII has been directly implicated in tubulointerstitial injury and fibrosis, [36-38]. Several studies showed that AII induces the expression of mesenchymal markers in experimental models of renal fibrosis. Johnson *et al.* showed that AII infusion resulted in tubular injury associated with *de novo* expression of  $\alpha$ -SMA and vimentin in renal interstitial cells [39]. In the rat proximal tubular cell line (NRK52-E), EMT was identified as a morphological change on epithelial cells from the typical cobblestone pattern to cells becoming elongated, along with reduced E-cadherin expression and synthesis of  $\alpha$ -SMA protein [40]. We demonstrated that the exposure of SHR PTCs to AII led to cell morphology modifications including the F-actin reorganization into stress fibers with increased focal adhesions and mesenchymal markers as  $\alpha$ -SMA and vimentin. Further, AII induced disruption of cell junctions, decreased E-cadherin and enhanced synthesis of MMP-9 and cell migration, being all these results consistent with a mesenchymal phenotype. However, SHR PTCs treated with (L) and (L+AII) formed epithelial cell monolayer with cuboidal morphology, typical of proximal tubular cells. Under these conditions, the polymerized F-actin formed a cortical ring around the cell periphery decreasing stress fibers and focal adhesions. Conversely, shHsp72 knockdown SHR PTCs treated with (L) and (L+AII), showed a phenotype similar to SHR PTCs without Losartan treatment.

The assembly and structural organization of actin cytoskeleton include the activation of small Rho GTPase proteins [41]. RhoA participates in some AII responses, including vasoconstriction, premyofibril formation and cell hypertrophy [4, 42]. A previous work demonstrated that activation of these Rho GTPases induced by AII, is a key step in the mesenchymal epithelial transition on proximal tubule cells [15]. In parallel, our results showed increased Rac1 and RhoA activation in AII treated SHR PTCs as well as in SHR PTCs control whereas the Losartan treatment in SHR PTCs induced decrease in Rac1 and RhoA activation. Although, in shHsp72 Knockdown SHR PTCs no significant changes were observed. According to these results, Rodriguez-Díez *et al.* [43] demonstrated that RhoA inhibition through transient transfection of a dominant negative RhoA or the use of ROCK inhibitors regulates AII-mediated EMT in AII treated human proximal tubule cells (HK2). Furthermore, in our study, (L) and (L+AII) treatment of SHR PTCs decreased vinculin levels and focal adhesion kinase (FAK) activation, while Losartan treated shHsp72 knockdown SHR PTCs showed an increase of both proteins. Taken together, these findings suggest that Hsp70 modulates Losartan effect blocking the AII action on actin cytoskeleton reorganization and focal adhesions formation.

Yang *et al.* [44] using a mouse unilateral ureteral obstruction model of severe renal fibrosis, described EMT in the kidney as an orchestrated process consisting of the classical four steps: loss of epithelial cell adhesion, *de novo* synthesis of  $\alpha$ -SMA, disruption of tubular basement membrane and cell migration and invasion. Evidence of EMT have also been reported in human diabetic and nondiabetic progressive nephropathies. In these renal pathologies, upregulation of renal renin-angiotensin system and tubular myofibroblast activation have been described [45, 46]. As well, rats that have been AII-infused for 2 weeks presented tubular damage and EMT induction demonstrated by  $\alpha$ -SMA upregulation and downregulation of E-cadherin [39]. We showed that AII treated SHR PTCs induced E-cadherin suppression and *de novo* vimentin and  $\alpha$ -SMA expression leading to epithelial cell adhesion loss and change from epithelial to fibroblast-like morphology. Nonetheless, these events were attenuated by SHR PTCs treatment with (L) or (L+AII). Conversely, in SHR PTCs after Hsp72 silencing, Losartan could not prevent the induction of events that lead to the EMT process. These results demonstrate that Losartan inhibits the AII induced-EMT of PTCs from hypertensive rats, and this effect is modulated by the Hsp70 chaperone.

*In vitro* and *in vivo* EMT induction is accompanied by increased expression of MMP-2 and MMP-9 metalloproteinases. Previous work showed that the incubation of matrigel,

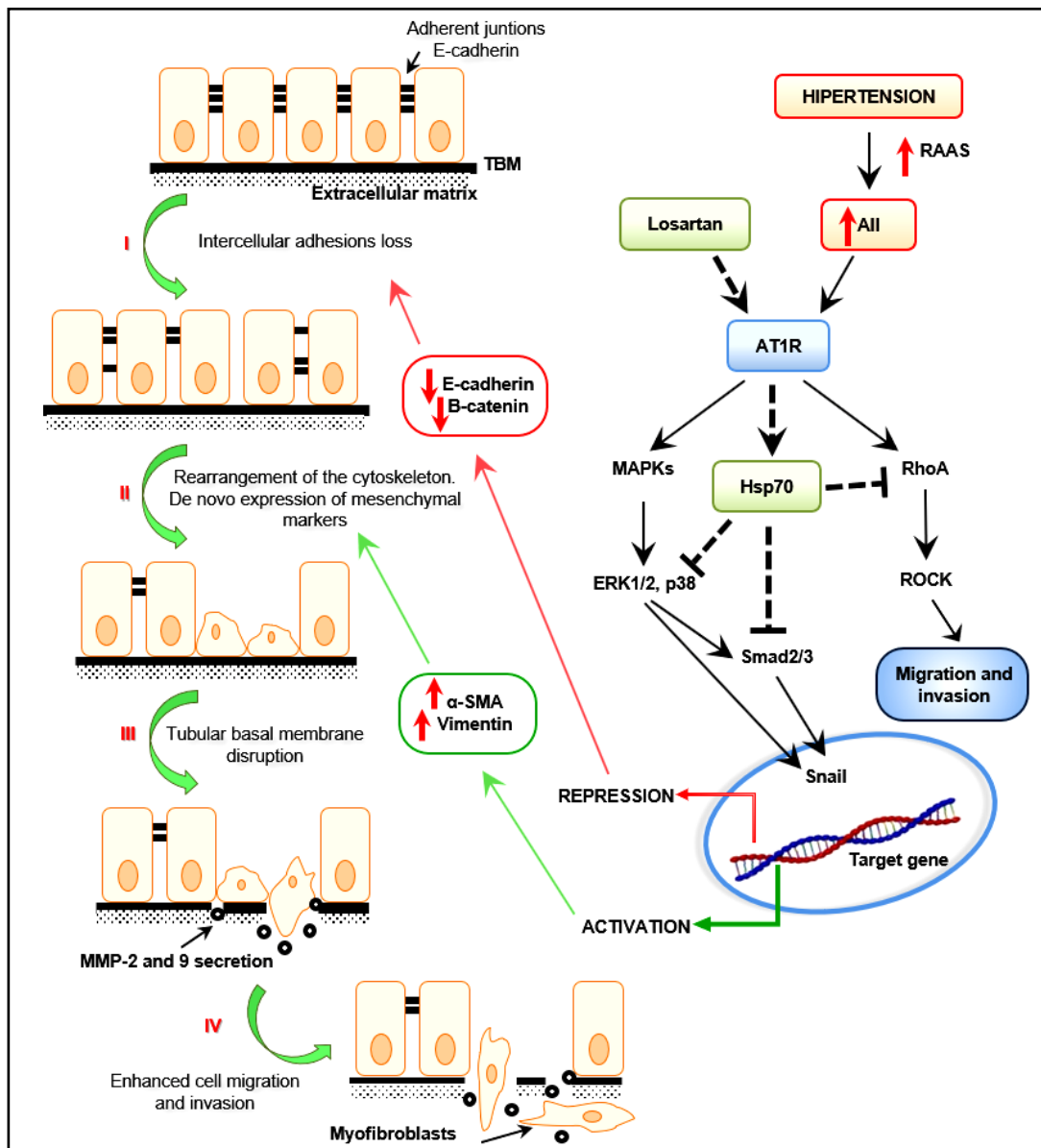


**Fig. 6.** Proposed mechanism by which Hsp70 mediates the negative regulation of EMT within Losartan effect in PTCs from SHR. Left panel: schematic illustration showing four key events during tubular epithelial cells to myfibroblast transition. Right panel: Throughout the activation of the MAPKs cascade and the RhoA/ROCK pathway, AII regulates EMT markers. The Hsp70 chaperone inhibits the signaling pathways that lead to EMT after Losartan AT<sub>1</sub> receptor blockage.

with conditioned media in transformed cells or tissue lysates from diseased kidneys results in destruction of its structural and functional integrity [44]. In agreement with this, our results from zymographic analysis of conditioned media showed that SHR PTCs control and AII treated exhibited a marked increase in MMP-2 and MMP-9 secretion, while Losartan treatment induced a significant reduction of these metalloproteinases. Despite, in SHR PTCs when Hsp72 expression was silenced, Losartan could not inhibit their secretion.

A previous publication showed that AII induces EMT by activating Smad signaling in the *in vivo* kidney and in cultured human tubule epithelial cells [16]. The regulation of E-cadherin expression is Smad 3 dependent, due to an increase of Snail1 expression [47, 48], whereas MMP-2 is regulated by Smad 2. Both Smad 2 and Smad 3 regulate  $\alpha$ -SMA [49].

In VSMCs, Smad 3 is involved in AII-mediated vascular fibrosis [18]. It has been shown that there is a cross-talk between MAPKs and Smad [12]. In vascular smooth muscle cells, AII activates Smad pathway via MAPKs activation [17]. We found that in SHR PTCs control and AII treated there were an increase in phosphorylated p38 and ERK MAPK levels as well as in phosphorylated Smad 2-3 indicating that AII induced EMT by MAPK/Smad 2-3 signaling pathway on SHR PTC. Yet, (L) and (L+AII) treatment significantly reduced p38, ERK, Smad 2-3 phosphorylation and Snail1 levels, these events are line with our previous results. Nevertheless, in SHR PTCs when Hsp72 expression was silenced, Losartan could not inhibit this pathway. These findings confirm that Losartan effect is modulated by Hsp70.

The phenotype switch from epithelial into mesenchymal cells involves acquisition of migratory properties. The reorganization of actin cytoskeleton, and induction  $\alpha$ -SMA, may provide a structural foundation not only for defining the morphology of the transformed cells but also for them to migrate, invade, and even to acquire contractile capacity [50, 51]. Our results showed that (L) and (L+AII) treatment in SHR PTCs induced a significant decrease on migration, cell displacement and movement velocity, while AII induced an increase of these events. However, the Losartan treatment in shHsp72 knockdown SHR PTCs show no changes on cell migration. Interestingly, we demonstrated that Losartan through Hsp70 maintains the intercellular junctions avoiding loss of cell-cell contact and changes in cell morphology.

Previously other authors have shown that induction of Hsp70 by nonlethal *in vitro* or *in vivo* insults is associated with acquired cytoprotection [52]. In the kidney, evidence from previous studies suggest that Hsp70 inhibits ischemic acute kidney injury [53, 54]. Our data indicate that Hsp70 is involved in the cellular response after AT<sub>1</sub> receptor blockage, inducing decreased profibrotic factors that lead to mesenchymal epithelium transition. Although the mechanism by which Hsp70 regulates p38, ERK and Smad 2-3 activation is unknown. A previous work showed that Hsp70 indirectly inhibits JNK (c-jun-N-terminal kinase) by preventing the inactivation of JNK-specific phosphatase during stress [55]. It may be suggested that Hsp70 could modulate phosphatases that regulate p38 and ERK thus, inhibiting the pathways that induced EMT. On the other hand, the induction of oxidative stress by AII may play a role in AII-induced EMT. Certainly, NADPH oxidase is directly activated by AII following activation of the AT<sub>1</sub> receptor [56]. Inhibition of ROS with antioxidants blocked EMT in tubular cells [57]. In a previous work, we demonstrated that Hsp70 mediates the ubiquitination and proteasomal degradation of Nox4 subunit of complex NADPH oxidase as part of the antioxidative effect of Losartan in SHR PTCs [22]. This is probably related to the effect observed in the EMT, however further studies are required to confirm it. The Fig. 6 schematizes the proposed mechanism by which Hsp70 inhibits EMT after AT<sub>1</sub> receptor blockage by Losartan.

## Conclusion

These results suggest a key role of Hsp70 on the AII induced EMT after AT<sub>1</sub>R blockage, being a possible molecular target for therapeutic strategy against hypertensive renal damage. Future *in vivo* investigations of Hsp70 participation in chronic renal diseases will allow us to design more effective combined therapeutic strategies to block the EMT process preventing renal interstitial fibrosis.

## Acknowledgements

We gratefully acknowledge Dr Michel Sherman, Boston University, Boston, MS, USA for kindly providing the shHsp72-pSIREN-RetroQ vector and pSIREN-RetroQ empty vector (mock transfection control).

This work was supported by grants from PICT-ANPCyT-CONICET 2016/1468 and 2016/1772 SECTYP UNCuyo. Resolution: No. 1720/2016-CS to V.V.Costantino and P.G. Vallés.

## Disclosure Statement

The authors have no conflicts of interests to declare.

## References

- 1 Lee LK, Meyer TW, Pollock AS, Lovett DH: Endothelial cell injury initiates glomerular sclerosis in the rat remnant kidney. *J Clin Invest* 1995;96:953-964.
- 2 Cuevas CA, Tapia-Rojas C, Cespedes C, Inestrosa NC, Vio CP: beta-Catenin-Dependent Signaling Pathway Contributes to Renal Fibrosis in Hypertensive Rats. *Biomed Res Int* 2015;2015:726012.
- 3 Ruperez M, Rodrigues-Diez R, Blanco-Colio LM, Sanchez-Lopez E, Rodriguez-Vita J, Esteban V, Carvajal G, Plaza JJ, Egido J, Ruiz-Ortega M: HMG-CoA reductase inhibitors decrease angiotensin II-induced vascular fibrosis: role of RhoA/ROCK and MAPK pathways. *Hypertension* 2007;50:377-383.
- 4 Ruiz-Ortega M, Ruperez M, Esteban V, Rodriguez-Vita J, Sanchez-Lopez E, Carvajal G, Egido J: Angiotensin II: a key factor in the inflammatory and fibrotic response in kidney diseases. *Nephrol Dial Transplant* 2006;21:16-20.
- 5 Dounousi E, Papavasiliou E, Makedou A, Ioannou K, Katopodis KP, Tselepis A, Siamopoulos KC, Tsakiris D: Oxidative stress is progressively enhanced with advancing stages of CKD. *Am J Kidney Dis* 2006;48:752-760.
- 6 Chabrashvili T, Tojo A, Onozato ML, Kitiyakara C, Quinn MT, Fujita T, Welch WJ, Wilcox CS: Expression and cellular localization of classic NADPH oxidase subunits in the spontaneously hypertensive rat kidney. *Hypertension* 2002;39:269-274.
- 7 Eddy AA: Molecular basis of renal fibrosis. *Pediatr Nephrol* 2000;15:290-301.
- 8 Stone RC, Pastar I, Ojeh N, Chen V, Liu S, Garzon KI, Tomic-Canic M: Epithelial-mesenchymal transition in tissue repair and fibrosis. *Cell Tissue Res* 2016;365:495-506.
- 9 Yanagita M: Antagonists of bone morphogenetic proteins in kidney disease. *Curr Opin Investig Drugs* 2010;11:315-322.
- 10 Okada H, Danoff TM, Kalluri R, Neilson EG: Early role of Fsp1 in epithelial-mesenchymal transformation. *Am J Physiol* 1997;273:F563-F574.
- 11 Liu Y: Epithelial to mesenchymal transition in renal fibrogenesis: pathologic significance, molecular mechanism, and therapeutic intervention. *J Am Soc Nephrol* 2004;15:1-12.
- 12 Ruiz-Ortega M, Rodriguez-Vita J, Sanchez-Lopez E, Carvajal G, Egido J: TGF-beta signaling in vascular fibrosis. *Cardiovasc Res* 2007;74:196-206.
- 13 Ellenrieder V, Hendler SF, Boeck W, Seufferlein T, Menke A, Ruhland C, Adler G, Gress TM: Transforming growth factor beta1 treatment leads to an epithelial-mesenchymal transdifferentiation of pancreatic cancer cells requiring extracellular signal-regulated kinase 2 activation. *Cancer Res* 2001;61:4222-4228.
- 14 Bakin AV, Rinehart C, Tomlinson AK, Arteaga CL: p38 mitogen-activated protein kinase is required for TGFbeta-mediated fibroblastic transdifferentiation and cell migration. *J Cell Sci* 2002;115:3193-3206.
- 15 Patel S, Takagi KI, Suzuki J, Imaizumi A, Kimura T, Mason RM, Kamimura T, Zhang Z: RhoGTPase activation is a key step in renal epithelial mesenchymal transdifferentiation. *J Am Soc Nephrol* 2005;16:1977-1984.
- 16 Carvajal G, Rodriguez-Vita J, Rodrigues-Diez R, Sanchez-Lopez E, Ruperez M, Cartier C, Esteban V, Ortiz A, Egido J, Mezzano SA, Ruiz-Ortega M: Angiotensin II activates the Smad pathway during epithelial mesenchymal transdifferentiation. *Kidney Int* 2008;74:585-595.
- 17 Rodriguez-Vita J, Sanchez-Lopez E, Esteban V, Ruperez M, Egido J, Ruiz-Ortega M: Angiotensin II activates the Smad pathway in vascular smooth muscle cells by a transforming growth factor-beta-independent mechanism. *Circulation* 2005;111:2509-2517.
- 18 Wang W, Huang XR, Canlas E, Oka K, Truong LD, Deng C, Bhowmick NA, Ju W, Bottinger EP, Lan HY: Essential role of Smad3 in angiotensin II-induced vascular fibrosis. *Circ Res* 2006;98:1032-1039.
- 19 Kalmar B, Greensmith L: Induction of heat shock proteins for protection against oxidative stress. *Adv Drug Deliv Rev* 2009;61:310-318.
- 20 Chebotareva N, Bobkova I, Shilov E: Heat shock proteins and kidney disease: perspectives of HSP therapy. *Cell Stress Chaperones* 2017;22:319-343.

- 21 Bocanegra V, Manucha W, Pena MR, Cacciamani V, Valles PG: Caveolin-1 and Hsp70 interaction in microdissected proximal tubules from spontaneously hypertensive rats as an effect of Losartan. *J Hypertens* 2010;28:143-155.
- 22 Costantino VV, Gil Lorenzo AF, Appiolaza ML, Cacciamani V, Benardon ME, Bocanegra V, Valles PG: Heat Shock Protein 70 and CHIP Promote Nox4 Ubiquitination and Degradation within the Losartan Antioxidative Effect in Proximal Tubule Cells. *Cell Physiol Biochem* 2015;36:2186-2197.
- 23 Gillis EE, Brinson KN, Rafikova O, Chen W, Musall JB, Harrison DG, Sullivan JC: Oxidative stress induces BH4 deficiency in male, but not female, SHR. *Biosci Rep* 2018;38:pii:BSR20180111.
- 24 Kurtz TW, Griffin KA, Bidani AK, Davisson RL, Hall JE: Recommendations for blood pressure measurement in humans and experimental animals. Part 2: Blood pressure measurement in experimental animals: a statement for professionals from the subcommittee of professional and public education of the American Heart Association council on high blood pressure research. *Hypertension* 2005;45:299-310.
- 25 Ikeda K, Nara Y, Yamori Y: Indirect systolic and mean blood pressure determination by a new tail cuff method in spontaneously hypertensive rats. *Lab Anim* 1991;25:26-29.
- 26 Pfeffer JM, Pfeffer MA, Frohlich ED: Validity of an indirect tail-cuff method for determining systolic arterial pressure in unanesthetized normotensive and spontaneously hypertensive rats. *J Lab Clin Med* 1971;78:957-962.
- 27 Helbert MJ, Dauwe SE, Van dB, I, Nouwen EJ, De Broe ME: Immunodissection of the human proximal nephron: flow sorting of S1S2S3, S1S2 and S3 proximal tubular cells. *Kidney Int* 1997;52:414-428.
- 28 Van dB, I, Nouwen EJ, Van Dromme SA, De Broe ME: Characterization of pure proximal and heterogeneous distal human tubular cells in culture. *Kidney Int* 1994;45:85-94.
- 29 Briones AM, Tabet F, Callera GE, Montezano AC, Yogi A, He Y, Quinn MT, Salaices M, Touyz RM: Differential regulation of Nox1, Nox2 and Nox4 in vascular smooth muscle cells from WKY and SHR. *J Am Soc Hypertens* 2011;5:137-153.
- 30 Liu Y, Rajur K, Tolbert E, Dworkin LD: Endogenous hepatocyte growth factor ameliorates chronic renal injury by activating matrix degradation pathways. *Kidney Int* 2000;58:2028-2043.
- 31 Kim TH, Mars WM, Stolz DB, Michalopoulos GK: Expression and activation of pro-MMP-2 and pro-MMP-9 during rat liver regeneration. *Hepatology* 2000;31:75-82.
- 32 Costantino VV, Mansilla SF, Speroni J, Amaya C, Cuello-Carrion D, Ciocca DR, Priestap HA, Barbieri MA, Gottifredi V, Lopez LA: The sesquiterpene lactone dehydroleucodine triggers senescence and apoptosis in association with accumulation of DNA damage markers. *PLoS One* 2013;8:e53168.
- 33 Xue M, Cheng Y, Han F, Chang Y, Yang Y, Li X, Chen L, Lu Y, Sun B, Chen L: Triptolide Attenuates Renal Tubular Epithelial-mesenchymal Transition Via the MiR-188-5p-mediated PI3K/AKT Pathway in Diabetic Kidney Disease. *Int J Biol Sci* 2018;14:1545-1557.
- 34 Yin J, Wang Y, Chang J, Li B, Zhang J, Liu Y, Lai S, Jiang Y, Li H, Zeng X: Apelin inhibited epithelial-mesenchymal transition of podocytes in diabetic mice through downregulating immunoproteasome subunits beta5i. *Cell Death Dis* 2018;9:1031.
- 35 Wang JY, Gao YB, Zhang N, Zou DW, Wang P, Zhu ZY, Li JY, Zhou SN, Wang SC, Wang YY, Yang JK: miR-21 overexpression enhances TGF-beta1-induced epithelial-to-mesenchymal transition by target smad7 and aggravates renal damage in diabetic nephropathy. *Mol Cell Endocrinol* 2014;392:163-172.
- 36 Mezzano SA, Ruiz-Ortega M, Egido J: Angiotensin II and renal fibrosis. *Hypertension* 2001;38:635-638.
- 37 Ruiz-Ortega M, Egido J: Angiotensin II modulates cell growth-related events and synthesis of matrix proteins in renal interstitial fibroblasts. *Kidney Int* 1997;52:1497-1510.
- 38 Border WA, Noble NA: Interactions of transforming growth factor-beta and angiotensin II in renal fibrosis. *Hypertension* 1998;31:181-188.
- 39 Johnson RJ, Alpers CE, Yoshimura A, Lombardi D, Pritzl P, Floege J, Schwartz SM: Renal injury from angiotensin II-mediated hypertension. *Hypertension* 1992;19:464-474.
- 40 Burns WC, Thomas MC: Angiotensin II and its role in tubular epithelial to mesenchymal transition associated with chronic kidney disease. *Cells Tissues Organs* 2011;193:74-84.
- 41 Kjoller L, Hall A: Signaling to Rho GTPases. *Exp Cell Res* 1999;253:166-179.
- 42 Lee DL, Webb RC, Jin L: Hypertension and RhoA/Rho-kinase signaling in the vasculature: highlights from the recent literature. *Hypertension* 2004;44:796-799.

- 43 Rodrigues-Diez R, Carvajal-Gonzalez G, Sanchez-Lopez E, Rodriguez-Vita J, Rodrigues DR, Selgas R, Ortiz A, Egido J, Mezzano S, Ruiz-Ortega M: Pharmacological modulation of epithelial mesenchymal transition caused by angiotensin II. Role of ROCK and MAPK pathways. *Pharm Res* 2008;25:2447-2461.
- 44 Yang J, Liu Y: Dissection of key events in tubular epithelial to myofibroblast transition and its implications in renal interstitial fibrosis. *Am J Pathol* 2001;159:1465-1475.
- 45 Mezzano S, Droguett A, Burgos ME, Ardiles LG, Flores CA, Aros CA, Caorsi I, Vio CP, Ruiz-Ortega M, Egido J: Renin-angiotensin system activation and interstitial inflammation in human diabetic nephropathy. *Kidney Int Suppl* 2003;S64-S70.
- 46 Mezzano SA, Aros CA, Droguett A, Burgos ME, Ardiles LG, Flores CA, Carpio D, Vio CP, Ruiz-Ortega M, Egido J: Renal angiotensin II up-regulation and myofibroblast activation in human membranous nephropathy. *Kidney Int Suppl* 2003;S39-S45.
- 47 Valcourt U, Kowanetz M, Niimi H, Heldin CH, Moustakas A: TGF-beta and the Smad signaling pathway support transcriptomic reprogramming during epithelial-mesenchymal cell transition. *Mol Biol Cell* 2005;16:1987-2002.
- 48 Han G, Wang XJ: Roles of TGFbeta signaling Smads in squamous cell carcinoma. *Cell Biosci* 2011;1:41.
- 49 Roberts AB, Tian F, Byfield SD, Stuelten C, Ooshima A, Saika S, Flanders KC: Smad3 is key to TGF-beta-mediated epithelial-to-mesenchymal transition, fibrosis, tumor suppression and metastasis. *Cytokine Growth Factor Rev* 2006;17:19-27.
- 50 Bar-Sagi D, Hall A: Ras and Rho GTPases: a family reunion. *Cell* 2000;103:227-238.
- 51 Krizbai IA, Bauer H, Amberger A, Hennig B, Szabo H, Fuchs R, Bauer HC: Growth factor-induced morphological, physiological and molecular characteristics in cerebral endothelial cells. *Eur J Cell Biol* 2000;79:594-600.
- 52 Kabakov AE, Budagova KR, Latchman DS, Kampinga HH: Stressful preconditioning and HSP70 overexpression attenuate proteotoxicity of cellular ATP depletion. *Am J Physiol Cell Physiol* 2002;283:C521-C534.
- 53 Wang Z, Gall JM, Bonegio RG, Havasi A, Hunt CR, Sherman MY, Schwartz JH, Borkan SC: Induction of heat shock protein 70 inhibits ischemic renal injury. *Kidney Int* 2011;79:861-870.
- 54 Basile DP, Donohoe D, Cao X, Van Why SK: Resistance to ischemic acute renal failure in the Brown Norway rat: a new model to study cytoprotection. *Kidney Int* 2004;65:2201-2211.
- 55 Havasi A, Li Z, Wang Z, Martin JL, Botla V, Ruchalski K, Schwartz JH, Borkan SC: Hsp27 inhibits Bax activation and apoptosis via a phosphatidylinositol 3-kinase-dependent mechanism. *J Biol Chem* 2008;283:12305-12313.
- 56 Griendling KK, Sorescu D, Ushio-Fukai M: NAD(P)H oxidase: role in cardiovascular biology and disease. *Circ Res* 2000;86:494-501.
- 57 Rhyu DY, Yang Y, Ha H, Lee GT, Song JS, Uh ST, Lee HB: Role of reactive oxygen species in TGF-beta1-induced mitogen-activated protein kinase activation and epithelial-mesenchymal transition in renal tubular epithelial cells. *J Am Soc Nephrol* 2005;16:667-675.